Monthly Notices of the ROYAL ASTRONOMICAL SOCIETY
MNRAS **498,** 1194–1204 (2020)
Advance Access publication 2020 August 6
doi:10.1093/mnras/staa2256

Self-consistent method to extract non-linearities from pulsating star light curves – I. Combination frequencies

M. Lares-Martiz ,⋆ R. Garrido⋆ and J. Pascual-Granado ⋆
Instituto de Astrofísica de Andalucía (IAA-CSIC), Glorieta de Astronomía s/n, 18008 Granada, Spain

Accepted 2020 July 24. Received 2020 July 24; in original form 2020 April 23

ABSTRACT

Stellar pulsation is a common phenomenon and is sustained because of coherent driving mechanisms. When pulsations are driven by heat or convective mechanisms, it is usual to observe combination frequencies in the power spectra of the stellar light-curves. These combination frequencies are not solutions of the perturbed stellar structure equations. In dense power spectra from a light-curve of a given multiperiodic pulsating star, they can compromise the mode identification in asteroseismic analyses, and hence they must be treated as spurious frequencies and removed. In this paper, a method based on fitting the set of frequencies that best describes a general non-linear model, like the Volterra series, is presented. The method allows these frequencies to be extracted from the power spectrum, thereby improving the frequency analysis and enabling hidden frequencies to emerge from what was initially considered as noise. Moreover, the method yields frequencies with uncertainties several orders of magnitude smaller than the Rayleigh dispersion, which is sometimes used as if it were an error when identifying combination frequencies. Furthermore, it is compatible with the classical counting cycles method, the so-called O-C method, which is valid only for mono-periodic stars. The method creates the possibility of characterizing the non-linear behaviour of a given pulsating star by studying in detail the complex generalized transfer functions on which the model is based.

Key words: asteroseismology – stars: oscillations – stars: variables: δ Scuti.

1 INTRODUCTION

Asteroseismology enables us to study stellar interiors by analysing and predicting pulsations, which travel at different depths depending on their frequency. The frequency content is typically obtained by a Fourier analysis. Sometimes, linear asteroseismic modelling cannot successfully explain the frequencies observed in the periodograms of pulsating stars, and this is the case for combination frequencies, which are commonly found in heat-driven pulsating stars such as RR Lyrae stars and Cepheids (e.g. Simon & Lee 1981), white dwarfs (e.g. Brickhill 1992; Zong et al. 2016), β Cepheids (e.g. Handler et al. 2006; Degroote et al. 2009), δ Sct stars (e.g. Balona et al. 2012; Bowman et al. 2016) and slowly pulsating B-type (SPB) stars (e.g. Pápics 2012; Kurtz et al. 2015), but which can also be seen in γ Dor stars (e.g. Kurtz et al. 2015; Saio et al. 2018), where the excitation mechanism is convective flux blocking.

Combination frequencies arise in the power spectra of some pulsating stars owing to the non-sinusoidal shape of their light-curves. Such particular changes in luminosity may have physical explanations related to mechanisms that follow non-linear dependences, such as the T^4 dependence in the Stefan–Boltzmann law for the emergent flux (e.g. Brassard, Fontaine & Wesemael 1995, who developed a theory for white dwarfs), or the non-linear response of the stellar interior to the oscillation wave (e.g. Gillet & Fokin 2014, who undertook a study of the propagation of shockwaves in RR Lyrae stars). In the literature, these possibilities for the physics of combination frequencies are generally referred to as *non-linear mixing processes* (Breger & Montgomery 2014) or gathered together in what is called the *non-linear distortion model* (Degroote et al. 2009; Bowman et al. 2016; Bowman 2017). In all cases, the consequences are non-linear interactions of the intrinsic pulsation modes of the star, which generate cross-terms at the summations, differences and harmonics of them.

Combination frequencies have been useful for mode identification in the asteroseismic analysis of ZZ Ceti stars (Wu 2001; Montgomery 2005). However, Balona (2012) demonstrated that the assumptions made for white dwarf theory are not valid for main-sequence pulsating stars such as δ Sct stars or β Cepheids. The reason is that geometrical effects (i.e. variations in the radius and surface normal) have to be taken into account, whereas these effects are negligible in white dwarfs, because of their high density. Therefore, because combination frequencies still have not proved to be useful for mode identification in main-sequence pulsating stars, and most likely become a source of confusion, they can be considered spurious frequencies and must be properly identified and removed from the power spectra.

Occasionally, combination frequencies are identified as such, for example when in a pre-whitening procedure the extracted frequency falls inside an ϵ range (usually the Rayleigh frequency resolution $\epsilon = 1/T$, where T is the observation interval) around a previously calculated exact combination value (Degroote et al. 2009; Pápics 2012; Murphy et al. 2013; Saio et al. 2018; Zwintz et al., in preparation). The inconsistency of this reasoning is that when the frequency does not match the value of the combination exactly, the residuals after the fit will be correlated with the thus-selected frequency. The techniques for the identification and extraction of combination frequencies explained in Handler et al. (2006), Balona et al. (2012) and Kurtz et al.

⋆ E-mail: mlm@iaa.es (MLM); garrido@iaa.es (RG); javier@iaa.es (JPG)

(2015) are more sophisticated than the aforementioned, taking into account that the fitted frequency must be the exact combination value.

In this paper, we present a novel self-consistent method for removing combination frequencies based on an unbiased estimation of the non-linear solution.The method aims to yield residuals uncorrelated with the frequencies generating these non-linearities. This is a continuation of Garrido & Rodriguez (1996), where, for the first time, the Volterra expansion was proposed as a mathematical framework to model the non-linearities present in some pulsating stars. An advantage of applying this method is that when the combination frequencies have been correctly removed from the time series, a new collection of frequencies, which were previously hidden, can emerge from the power spectra. In addition, the method can provide frequency errors that are much more realistic than the coarse estimations given by the Rayleigh frequency resolution.

The paper is organized as follows. Section 2 provides the theoretical basis. Section 3 presents a detailed description of the methodology. The results of applying this technique to various light-curves are given in Section 4, and the results are discussed in Section 5. Finally, Section 6 summarizes the conclusions drawn from this study and suggests directions for future work.

2 THEORETICAL BASIS: GENERAL RESPONSE OF A NON-LINEAR SYSTEM

Non-linear systems can be studied and represented by the Volterra series. In the particular case where the input to a non-linear system is a single real-valued sine wave at ω_0 with amplitude A_0, the output can be expressed (see Priestley 1988, p. 29) as

$$\begin{aligned} Y(t) = {} & A_0\,\Gamma_1(\omega_0)\,\mathrm{e}^{\mathrm{i}\,\omega_0\,t+\phi_0} + A_0^2\,\Gamma_2(\omega_0,\omega_0)\,\mathrm{e}^{2\,\mathrm{i}\,\omega_0\,t+2\,\phi_0} \\ & + A_0^3\,\Gamma_3(\omega_0,\omega_0,\omega_0)\,\mathrm{e}^{3\,\mathrm{i}\,\omega_0\,t+3\,\phi_0} + \ldots, \end{aligned} \tag{1}$$

where the Γ_j functions are the generalized transfer complex functions. Subindexes denote the non-linear order of interactions; that is, Γ_1 represents the system response for each independent frequency, Γ_2 represents the system response for first-order interactions, and so on.

The generalized transfer functions Γ_j can be written as a Volterra expansion. These series, although they retain some of the system memory, are non-orthogonal. To disentangle the correlation between the basis functionals of the Volterra series, the Wiener orthogonal expansion (Wiener 1958) can be used. The final intention is to obtain a physical model that explains non-linearities. In this paper, the orthogonality of expression (1) is assumed, enabling the study of certain properties that can be observed in a first-order approximation.

Although *Y(t)* is not linear between the input/output spectra, it is linear between *Y(t)* and the Γ_j (Scargle 2020), so a standard least-squares procedure quantifies not only the parameters of the input components, but also the contribution from the generalized transfer functions. For example, because the Γ_j functions are complex functions, equation (1) can be rearranged as

$$Y(t) = \tilde{A}_1\,\mathrm{e}^{\mathrm{i}\omega_0\,t+\tilde{\phi}_1} + \tilde{A}_2\,\mathrm{e}^{2\,i\,\omega_0\,t+\tilde{\phi}_2} + \tilde{A}_3\,\mathrm{e}^{3\,\mathrm{i}\,\omega_0\,t+\tilde{\phi}_3} + \ldots, \tag{2}$$

where

$$\begin{aligned} \tilde{A}_1 &= A_0\,|\Gamma_1(\omega_0)|, \\ \tilde{A}_2 &= A_0^2\,|\Gamma_2(\omega_0,\omega_0)|, \\ \tilde{A}_3 &= A_0^3\,|\Gamma_3(\omega_0,\omega_0,\omega_0)| \end{aligned} \tag{3}$$

and

$$\begin{aligned} \tilde{\phi}_1 &= \phi_0 + \arg\{\Gamma_1(\omega_0)\}, \\ \tilde{\phi}_2 &= 2\,\phi_0 + \arg\{\Gamma_2(\omega_0,\omega_0)\}, \\ \tilde{\phi}_3 &= 3\,\phi_0 + \arg\{\Gamma_3(\omega_0,\omega_0,\omega_0)\}. \end{aligned} \tag{4}$$

Examining the case when the input is composed of two real-valued sine waves at frequencies ω_0 and ω_1, the output of a non-linear system modelled by a Volterra series is

$$\begin{aligned} Y(t) = {} & A_0\,\Gamma_1(\omega_0)\,\mathrm{e}^{\mathrm{i}\,\omega_0\,t+\phi_0} + A_1\,\Gamma_1(\omega_1)\,\mathrm{e}^{\mathrm{i}\,\omega_1\,t+\phi_1} \\ & + A_0^2\,\Gamma_2(\omega_0,\omega_0)\,\mathrm{e}^{2\,\mathrm{i}\,\omega_0\,t+2\,\phi_0} + A_1^2\,\Gamma_2(\omega_1,\omega_1)\,\mathrm{e}^{2\,\mathrm{i}\,\omega_1\,t+2\,\phi_1} \\ & + A_0\,A_1\,\Gamma_2(\omega_0,\pm\omega_1)\,\mathrm{e}^{\mathrm{i}\,(\omega_0\pm\omega_1)\,t+(\phi_0\pm\phi_1)} \\ & + A_1\,A_0\,\Gamma_2(\omega_1,\pm\omega_0)\,\mathrm{e}^{\mathrm{i}\,(\omega_1\pm\omega_0)\,t+(\phi_1\pm\phi_0)} + \ldots. \end{aligned} \tag{5}$$

Equation (5) can be rearranged as

$$\begin{aligned} Y(t) = {} & \tilde{A}_1\,\mathrm{e}^{\mathrm{i}\omega_0\,t+\tilde{\phi}_1} + \tilde{A}_2\,\mathrm{e}^{\mathrm{i}\,\omega_1\,t+\tilde{\phi}_2} + \tilde{A}_3\,\mathrm{e}^{2\,\mathrm{i}\,\omega_0\,t+\tilde{\phi}_3} \\ & + \tilde{A}_4\,\mathrm{e}^{2\,\mathrm{i}\,\omega_1\,t+\tilde{\phi}_4} + \tilde{A}_5\,\mathrm{e}^{\mathrm{i}\,(\omega_0\pm\omega_1)\,t\pm\tilde{\phi}_5} + \ldots, \end{aligned} \tag{6}$$

where

$$\begin{aligned} \tilde{A}_1 &= A_0|\Gamma_1(\omega_0)|, \\ \tilde{A}_2 &= A_1|\Gamma_1(\omega_1)|, \\ \tilde{A}_3 &= A_0^2|\Gamma_2(\omega_0,\omega_0)|, \\ \tilde{A}_4 &= A_1^2|\Gamma_2(\omega_1,\omega_1)|, \\ \tilde{A}_5 &= A_0A_1|\Gamma_2(\omega_0,\omega_1)|, \\ \text{or } \tilde{A}_5 &= A_1A_0|\Gamma_2(\omega_1,\omega_0)|^{\dagger} \end{aligned} \tag{7}$$

and

$$\begin{aligned} \tilde{\phi}_1 &= \phi_0 + \arg\{\Gamma_1(\omega_0)\}, \\ \tilde{\phi}_2 &= \phi_1 + \arg\{\Gamma_1(\omega_1)\}, \\ \tilde{\phi}_3 &= 2\,\phi_0 + \arg\{\Gamma_2(\omega_0,\omega_0)\}, \\ \tilde{\phi}_4 &= 2\,\phi_1 + \arg\{\Gamma_2(\omega_1,\omega_1)\}, \\ \tilde{\phi}_5 &= \phi_0 \pm \phi_1 + \arg\{\Gamma_2(\omega_0,\pm\omega_1)\}, \\ \text{or } \tilde{\phi}_5 &= \phi_1 \pm \phi_0 + \arg\{\Gamma_2(\omega_1,\pm\omega_0)\}^{\dagger}. \end{aligned} \tag{8}$$

A Fourier transform of equation (6) would result in a power spectrum with peaks at the independent frequencies ω_0 and ω_1 (called the parent frequencies in this paper), as well as at the frequencies of the non-linear terms, which are the combination frequencies (called children in this paper). This is a well-known phenomenon in system and signal analysis and is known as *intermodulation distortion*. In the case of one parent frequency, it is called *frequency multiplication* or *harmonic distortion*.

Modelling non-linearities by treating the variable star as a non-linear but stationary system is the mathematical foundation for the method presented here. We are assuming a known input equal to a basic harmonic signal.

3 METHODOLOGY: THE 'BEST' PARENTS

Under the hypothesis that equations (2) and (6) are approximation functions modelling the non-linearities present in the light-curves of mono-periodic and double-mode variable stars, respectively, a least-squares fit of them should yield residuals uncorrelated with the combination frequencies. The variance of such residuals (in comparison with the variance of the original light-curve) quantifies

†Because no condition of symmetry is yet imposed.

to what extent the parents and children fitted explain the signal as non-linearities: the lower the variance value, the better the fit.

We define V as the continuous function of the variance related to different fittings of parent frequencies (and their statistically significant combinations) to a given light-curve. Therefore, V is a function only of the parent frequencies. The aim is to find a minimum in V. There are several procedures for finding the minimum in a non-linear least-squares fitting (when the fitted functions are non-linear in the parameters) (Bevington & Robinson 2003), but in the method presented here we follow an empirical approach, which consists of exploring the n-dimensional surface of independent frequencies. First, we fit several sets of children whose parents differ in a small frequency step (the number of sets and the size of the steps are parameters that can be chosen by the user of the algorithm; here we explore five sets starting with a step of 0.1 d^{-1}). When a set of parents that minimizes the residuals is found in an iteration, these parents act as seeds for the next iteration, in which the search is conducted with a smaller step (with the next lower magnitude order: 0.01 d^{-1}). The advantage of this empirical minimization is that it ensures an exhaustive search for the 'best' parents.

In the case of a single parent frequency (e.g. a Cepheid or a high-amplitude mono-periodic variable), we select the highest peak in the power spectrum as a first approximation to the parent frequency with a coarse precision. Then, $V(\omega)$ is sampled with a progressively smaller step until the minimum is reached. In this way, the minimum V value gives us a much more precise frequency. Often, the frequency error is smaller than the Rayleigh dispersion. As we will see in Section 4.1, the frequency value is compatible with that obtained by the O-C (Observed minus Calculated) method (Sterken 2005), which is basically how the times of arrival of the pulses are determined in the pulsar timing analysis technique, known for yielding extraordinary precision when calculating the period of a pulsar (Lorimer & Kramer 2004).

Now that we know the 'best' parent frequency, in the case of a single parent mode, we calculate the set of combinations (in this case, harmonics) not exceeding the Nyquist frequency, to test whether they are statistically significant, by applying any statistical test (e.g. Student's t or Snedecor's F). It is important to highlight that the applicability of this method is not just for evenly spaced data. When dealing with unequally spaced data, the set of combinations to calculate and fit can be accordingly chosen up to any convenient frequency.

In the case of two parent frequencies, for example double-mode Cepheids, high-amplitude δ Sct (HADS) stars or RR Lyrae stars, or multiperiodic stars such as low-amplitude δ Sct (LADS) stars, γ Dor, etc., the procedure is the same as for finding the 'best' parents, but for calculating all the combination values we use the form

$$\omega_k = \left|\pm n\,\omega_i \pm m\,\omega_j\right|, \tag{9}$$

where m and n are integer numbers under the condition that the ω_k do not exceed the Nyquist frequency. The absolute sum of n and m defines the combination order. We choose to limit equation (9) to a two-termed expression to avoid increasing the probabilities for false identifications. A fit to the light-curve of all the calculated combinations and their parents is computed. In this paper, a Student's t criterion of significance with a level of confidence of 99.9 per cent is used. Finally, depending on whether the initial data are evenly or unevenly spaced, a fast Fourier transform (FFT) or Lomb–Scargle (LS) periodogram, respectively, of the residual light-curve results in a power spectrum free of combination frequencies, which is the aim of this work.

In summary, the method consists essentially of two steps. The first is the 'standard' approach of fitting sinusoids to the light-curve (but under the framework given in Section 2), optimizing the frequency, amplitude and phase using non-linear least squares (but with a minimization that ensures an exhaustive testing of the possible parents). This yields the parent frequencies that best describe the signal's non-linearities (we call this first step the 'best' parent method, BPM, from now on). The second step is fitting them together with the set of children frequencies originating from them.

4 RESULTS

Although this non-linearity analysis applies to every type of pulsator with combination frequencies, we focused on δ Sct stars owing to their dense and unexplained power spectra (Poretti et al. 2009; Mantegazza et al. 2012; García Hernández et al. 2013). To test the performance of the method, three δ Sct stars, of different pulsational contents, were chosen: first, a mono-periodic δ Sct variable, in order to verify the process of finding the 'best' parent; next, a double-mode pulsator; and finally, a multiperiodic δ Sct star, where more complex non-linearities can be present and where their extraction could be critical to the frequency analysis. Details of the physical parameters and relevant information describing the light-curves are listed in Table A1, located in Appendix A.

It is known that gaps in time series are a source of uncertainties and error in harmonic analysis; see for instance Pascual-Granado et al. (2018). Therefore, gaps in the light-curves used in this

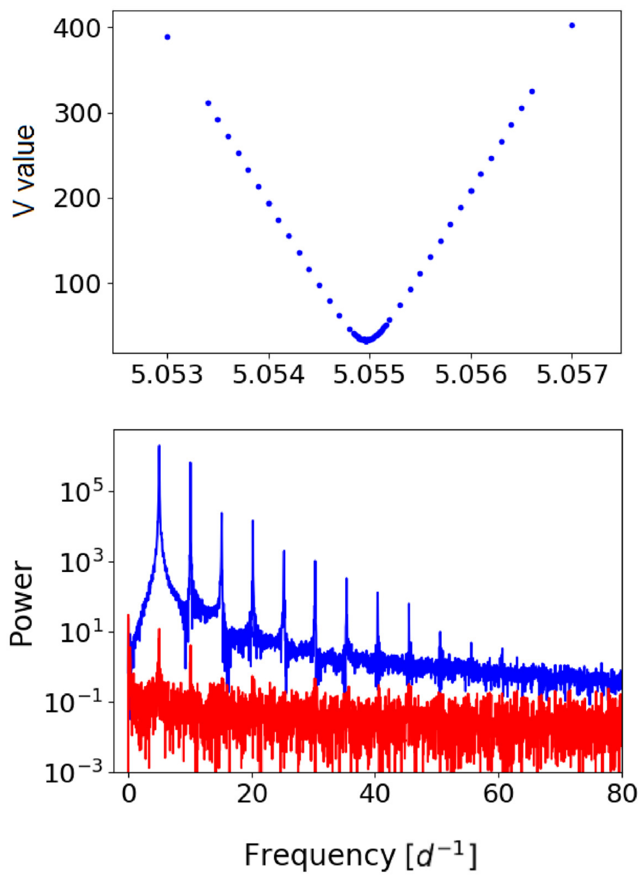

Figure 1. Application of the BPM to the light-curve of TIC 9632550. Upper panel: fundamental period found as a local minimum at 5.054963644 d^{-1}. Lower panel: in blue, the FFT of the original light-curve; in red, the FFT of the residuals after fitting the fundamental frequency and 13 statistically significant harmonics.

Table 1. The 'best' parent search tree for the mono-periodic δ Sct star TIC 9632550. The first column quantifies the number of statistically significant frequencies, or children, detected with the parent frequency specified in the third column, in d^{-1} (zeros are omitted for the sake of clarity). The second column is the variance after fitting the parent and combination frequencies (in this case, only harmonics of the highest one).

No. of fitted frequencies	V value	Frequency [d^{-1}]
1	3155.844405793707201	5.0
5	948.937738175725485	5.05
14	33.629889361388315	5.055
14	33.629889361388315	5.055
14	**32.871889584474623**	**5.05496**
14	32.862102488776905	5.054964
14	32.862102488776905	5.054964
14	32.862101660828912	5.05496404
14	32.862101656257245	5.054964037
14	32.862101656225789	5.0549640372
14	32.862101656224368	5.05496403722
14	32.862101656224311	5.054964037229
14	32.862101656223409	5.0549640372274
14	32.862101656222627	5.05496403722726
14	32.862101656222627	5.05496403722726

study were filled using the MIARMA (Method of Interpolation with AutoRegressive Moving Average) algorithm (Pascual-Granado, Garrido & Suárez 2015), which aims to remove the effects of the observational window while preserving the frequency content of the star. When the gap is sufficiently small (in the KIC 5950759 *Kepler* light-curve, for example, only a few points are missing), then a linear interpolation is sufficient.

4.1 Mono-periodic stars: the δ Sct case

The method applied to a light-curve of a mono-periodic pulsating star results in a local minimum of the V function, which determines the fundamental period. This is shown for the mono-periodic δ Sct star TIC 9632550 (Fig. 1, upper panel), observed by the Transiting Exoplanet Survey Satellite (TESS, Ricker et al. 2014).

The iterative process of searching for the 'best' parent, explained in Section 3, refines the frequency until the variance value (V) does not change. In this particular case, this happened at the 14th iteration (see Table 1). However, we chose the value at the 5th iteration (see the discussion in Section 5.1 for a full explanation). Our result for the fundamental frequency is compatible with the one obtained by the O-C procedure (see Fig. 2),

$$\omega_0 = (5.05496 \pm 0.00002)\,\mathrm{d}^{-1}.$$

The FFT of the residual light-curve after fitting the fundamental frequency and its harmonics is almost cleaned from all signal contribution. This is graphically represented in the lower panel of Fig. 1 and quantitatively expressed by the high percentage of the original power explained by these non-linear effects and their parents (expressed as %CF in Table 2). There are, however, three peaks remaining in the residual power spectrum: the first one corresponds to the first frequency bin and is the residual of a second-order polynomial fitting performed in order to remove any trend in the light-curve; the second peak, appearing next to the fundamental frequency, and the third one, which is next to the first harmonic, are possibly explained by an amplitude modulation of the fundamental frequency. An alternative explanation for why these two peaks appear at about the same frequencies as the fitted ones might be the fractal property studied by De Franciscis et al. (2018), which is impossible to reproduce by using a Fourier representation. In any case, the logarithmic scale shows five orders of magnitude difference between the original and the residual power, which is in very good agreement with our expectation of uncorrelated residuals.

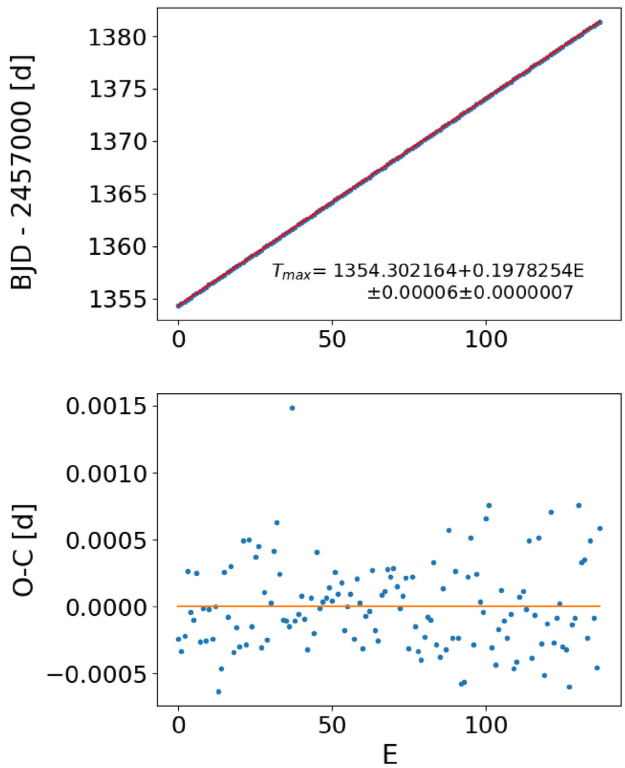

Figure 2. Application of the O-C method to the light-curve of TIC 9632550. Upper panel: in blue, the times of the light maximum, corresponding to the maximum value of a parabola fitted to each cycle; in red: the regression line $T_{\max} = T_0 + PE$, where P is the trial period, T_0 is the zero epoch, and E is an integer number of cycles elapsed since the zero epoch. The fundamental frequency ($\omega_0 = 1/P$) calculated by the O-C method is $\omega_0 = (5.05496 \pm 0.00002)\ \mathrm{d}^{-1}$. Lower panel: residuals of the regression.

Table 2. Results of the combination frequencies extraction process for the mono-periodic δ Sct star TIC 9632550. The first column show the 'best' parent from the search tree in cycles per day. The second column specifies the number of statistically significant frequencies, or children, extracted. The %CF (third column) quantifies the percentage of the initial power attributable to the combination frequencies and their parents.

	TIC 9632550		
Tag	'Best' parent [d^{-1}]	Combinations extracted	%CF
f0	5.05496	13 harmonics	98.98

4.2 Double-mode stars: the HADS case

We now extend the procedure described in the previous section for the 'best' parent search to double-mode stars.

There is a slight tendency for HADS stars to have higher number of non-linearities (Balona 2016). This is why we chose to apply the method to KIC 5950759, a HADS star observed by the *Kepler* satellite (Gilliland et al. 2010) whose non-linearities were first studied by Bowman (2017). The original power spectrum (blue in Fig. 3) shows a very regular structure, where the first two highest peaks

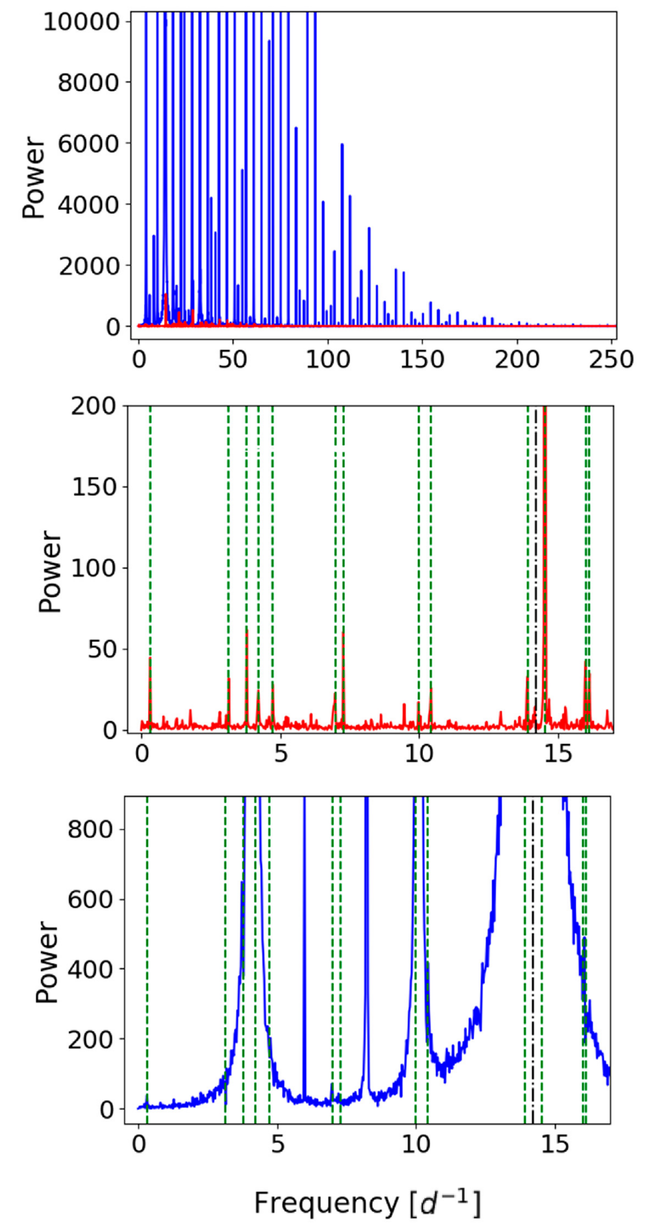

Figure 3. Application of the BPM to the light-curve of KIC 5950759. Blue: FFT of the original light-curve. Red: FFT of the residuals after fitting the 'best' parents and the combinations generated by them. Green dashed: new frequencies detected in the residuals of the fitting. Black dash–dotted: 'best' parent frequencies. Notice in the middle panel the significant peak corresponding to $\omega_{\mathrm{m}} \approx 0.32\ \mathrm{d}^{-1}$. Also notice that the separation between the dashed green lines around the black dash–dotted line is equal to ω_{m}.

follow the fundamental period and the first overtone ratio expected to occur for δ Sct stars (see Stellingwerf 1979).

In a recent study for this star by Yang et al. (2018), the parent frequencies for the short-cadence (SC) data were

$$\omega_0 = (14.221367 \pm 0.000015)\ \mathrm{d}^{-1},$$
$$\omega_1 = (18.337228 \pm 0.000023)\ \mathrm{d}^{-1},$$

which are compatible with the 'best' parents computed by the BPM (see Table 3). In Yang et al. (2018), frequency errors were calculated according to a heuristically derived formula for the upper limit of the frequency uncertainty in Kallinger, Reegen & Weiss (2008). The

Table 3. Results of the combination frequencies extraction process for the double-mode HADS star KIC 5950759. The first column show the 'best' parents from the search tree in cycles per day. The second column specifies the number of statistically significant frequencies, or children, extracted. The %CF (third column) quantifies the percentage of initial power attributable to the combination frequencies and their parents.

	KIC 5950759		
Tag	'Best' parents [d^{-1}]	Combinations extracted	%CF
f0	14.22136	177 in total:	97.48
f1	18.33722	17 harmonics	
		92 sums	
		and 68 differences	

precision reached with the 'best' parents search is also empirically justified in Section 5.1.

As a result of the high power of the initial components, the limit for considering a combination frequency to be significant was too high, leaving components of children frequencies in the signal. That is why we continued the extraction of frequencies from the residual light-curve, a process that was completed in three steps. In the first fit, 71 combinations were significant (black in Fig. 4); in the second, 99 (green in Fig. 4); and finally, 7 (red in Fig. 4). Notice how the black FFT still has many significant combination frequencies (in the range of 160 and 300 d^{-1}), which justifies the subsequent fits. The green FFT is almost completely covered, because it is practically the same as the red one (only seven frequencies, of small amplitude, are different). As a consequence of these fittings, a new frequency structure (which was previously hidden) emerges in the power spectrum (see the middle panel of Fig. 3). Notice that the frequency $\omega_{\mathrm{m}} \approx 0.32\ \mathrm{d}^{-1}$, which is modulating the entire spectrum, is now significant according to the Reegen (2007) criterion of signal/noise $>$12.57 in the power domain.

As first discussed by Bowman (2017), the new frequency structure seen for KIC 5950759 deserves further study regarding its origin, because it could possibly indicate the existence of other independent modes. Yang et al. (2018) explored several physical explanations, proposing the most likely as identifying ω_{m} with the rotation of the star, meaning that the dashed lines around ω_0 in the middle panel of Fig. 3 correspond to the modulation of the main pulsation modes with the rotation frequency. Other possible explanations for the fine structures appearing around the main frequencies might be carefully evaluated taking into account the work of Zong et al. (2018), where different frequency and/or amplitude modulation patterns were identified in the power spectra of an ensemble of pulsating hot B subdwarf (sdB) and white dwarf stars observed by the *Kepler* satellite.

In any case, the results shown in Fig. 3 provide a new level of relevance to this method: with a correct extraction of the combination frequencies, like the one proposed in this work, it is possible to unveil frequency structures that previously did not exceed the detection threshold. In this particular case, we were able to detect the ω_{m} frequency using SC data, while in Yang et al. (2018) long-cadence (LC) data, a super-Nyquist and alias analysis were necessary in order to identify it.

4.3 Multiperiodic stars: the LADS case

For more than two parents, exploring the frequency space of the V function recursively to find its minimum value can be computationally expensive, but the implications of applying the BPM can be crucial for an asteroseismic analysis, as we showed in the previous section. We applied the method to the light-curve of HD 174966

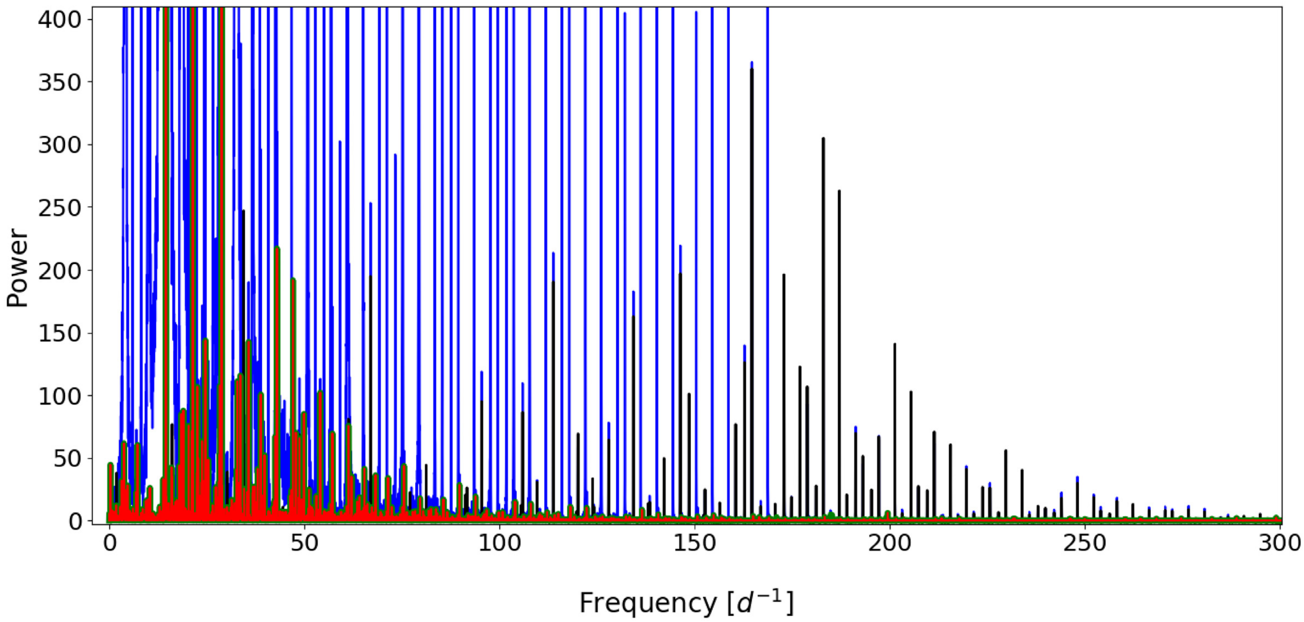

Figure 4. Extraction of non-linearities by groups for KIC 5950759. The power spectra of the residuals after fitting each group of frequencies are colour-coded: blue corresponds to the original light-curve, black to the residuals after fitting the first group of frequencies (71 children), green to the residual light-curve obtained after fitting the second group of frequencies (99 children), and red to the residual light-curve after fitting the last group of frequencies (7 children).

Table 4. The BPM for every possible couple of the first five highest power peaks in the HD 174966 power spectrum.

Couple tag	Couple frequencies $[d^{-1}]$
(f0, f1)	(17.62288, 23.19479)
(f0, f2)	(17.62298, 21.42079)
(f0, f3)	(17.62280, 26.95853)
(f0, f4)	(17.62291, 27.71456)
(f1, f2)	(23.19477, 21.42097)
(f1, f3)	(23.19479, 26.95851)
(f1, f4)	(23.19477, 27.71503)
(f2, f3)	(21.42078, 26.95853)
(f2, f4)	(21.42078, 27.71463)
(f3, f4)	(26.95851, 27.71487)

Table 5. Results of the combination frequencies extraction process for the multimode δ Sct star HD 174966. The first column show the 'best' parents from the search tree in d^{-1}. The second column specifies the number of statistically significant frequencies, or children, extracted. The %CF (third column) quantifies the percentage of the initial power resulting from the combination frequencies and their parents.

	HD 174966		
Tag	'Best' parents $[d^{-1}]$	Combinations extracted	%CF
f0	17.6230	118 in total:	93.01
f1	23.1948	1 harmonic	
f2	21.4210	11 sums	
f3	26.9585	106 differences	
f4	27.7150		

(see Fig. 5), a LADS star (or simply a δ Sct star) observed by the *CoRoT* satellite (Auvergne et al. 2009). This star was studied by García Hernández et al. (2013), who found that the 5th highest peak in the amplitude spectrum was very near to the estimated fundamental radial mode (17.3 ± 2.5 d^{-1}).

Therefore, we chose as independent frequencies the first five peaks of highest power, but, instead of searching the combinations of the full set of five independent frequencies, we decided to divide the search into couples in order to reduce the computational cost of the BPM solution. In Table 4, the results of the BPM for every possible couple with the precision adopted in this work (see Section 5.1) show small differences. In this case, we select as the 'best' parents for the five highest-amplitude peaks the values with the best precision in which they are compatible in each search.

Particularly in this star, 118 combinations were statistically significant (see Table 5). Notice that the number of differences is higher than the number of sum combinations. This may raise concerns about the validity of these identifications in the lower frequency range. The majority of these differences correspond to high-order combinations (see Table B3), but harmonics ($n\omega_i$ or $m\omega_j$) with such high n and m are not statistically significant (only 2f3 is detected). Alternatively, these significant differences could simply be false identifications owing to the fact that at higher n and m more combinations are tested, increasing the probability of a match, as well as the possibility of choosing as parent frequencies a combination frequency. In this work, we do not exclude any match because we are interested in finding the set of combination frequencies that could explain the most of the signal as non-linearities. Furthermore, Kurtz et al. (2015) state that the amplitude of a child frequency could be higher than their parents' amplitudes, which could explain the missing high-order harmonics issue.

Further discriminating criteria (apart from the frequency value) are required for an unambiguous identification, so as to avoid false identifications due to high values of n and m. Nevertheless, this example shows that in no case is the method introducing new frequencies, and that even when it is not clear that the arbitrarily chosen parent frequencies are actual oscillation modes of the star (which is often the case when dealing with multiperiodic stars), the set of significant combinations resulting from the algorithm can still be useful to test whether extracting them has simplified the power spectrum in agreement with a solution from a linear stellar oscillation model (see Fig. 5, where some of the green

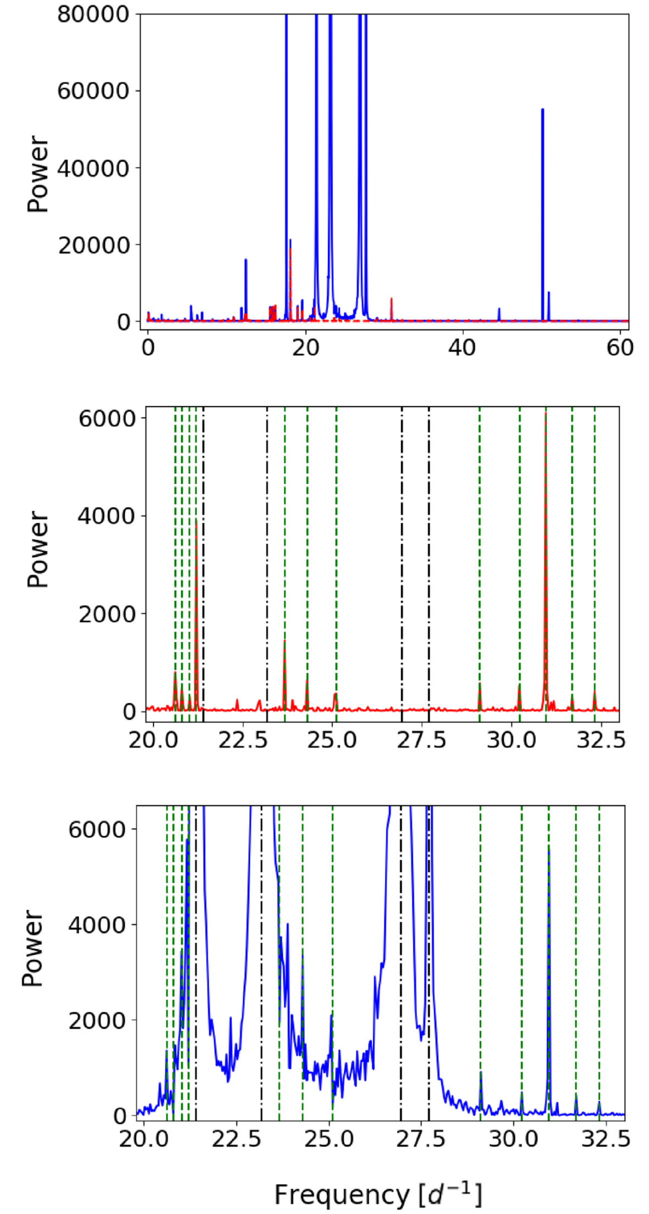

Figure 5. Application of the BPM to the light-curve of HD 174966. Blue: FFT of the original light-curve. Red: FFT of the residuals after fitting the 'best' parents and the series of combinations originating from them. Green dashed: new frequencies detected after the fit. Black dash–dotted: 'best' parent frequencies.

dashed lines are equally spaced, possibly identifiable with non-radial frequency structures or rotational splittings). This is again showing that extracting combination frequencies in a least-squares sense, as a first step before undertaking the frequency analysis, can expose pulsation modes or frequency spacing patterns in which we are interested, and that would otherwise be hidden.

5 DISCUSSION

We consider spurious peaks as significant and non-significant maxima in the frequency spectrum that do not correspond to any oscillation mode of the pulsating star (Suárez et al. 2020). In this sense, peaks associated with non-linear effects should not be considered spurious because they originate in the oscillations themselves. However, no closed-form formulae like, for instance, equations (1) and (5), have been obtained so far to characterize these non-linear effects. Therefore, until such expressions are developed, we can consider non-linear components appearing in the frequency spectrum as spurious peaks.

In this paper, we have introduced a mathematical formalism for the non-linear solution of multiperiodic pulsating stars based on the expansion in a Volterra series through equations (2) to (8). Notice that the generalized transfer functions do not influence the frequencies, the topic of this first part of the overall study. What is relevant in this formulation for the present paper is that this output could describe the rapid increases and slow decreases of the luminosity observed in some light-curves. On the other hand, the amplitude and phase relationships appearing in those equations are considerably different from the ones suggested by the so-called *simple model* in Breger & Montgomery (2014). An analysis of amplitude and phase relationships affected by the Γ_j functions (equations 3, 7 and 4, 8 for the mono-periodic and double-mode cases, respectively) will be undertaken in a future publication.

A combination frequency could not correspond to an interaction between modes owing to their intrinsic non-linear behaviour. It could be a new unstable mode (very near the exact combination frequency value) that undergoes amplitude enhancement as a result of the resonance mode coupling mechanism (Dziembowski 1982; Dziembowski & Krolikowska 1985; Dziembowski, Krolikowska & Kosovichev 1988; Van Hoolst 1994). It is important to investigate this possibility because it could clarify why stars with similar parameters exhibit very different power spectra (Balona & Dziembowski 2011). In this paper, we focus on discriminating combination frequencies from oscillation modes of the star only by the frequency relationship between parents and children (equation 9). However, pulsation modes could still have the same frequency value as a combination by chance, and this possibility is the main limitation of this method.

In Section 3 we described the BPM, the procedure to find the optimal frequencies in the non-linear least-squares fitting used in this work. Computationally, it could be time-consuming for stars for which there is no prior knowledge regarding which could be the parent modes (e.g. δ Sct stars, γ Dor), where more than two frequencies have to be taken as possible parents. Despite this, the BPM is transparent and has the potential to find the frequencies that best describe the set of non-linearities in the data. Thus, no frequency values (and their combinations) are left untested. The parameters used for this systematic search (i.e. the number of steps around the initial value and the length of this step) determine the computation time, as well as the goodness of the optimization.

In practice, frequencies extracted from a pre-whitening cascade are identified as a combination when they fall inside a Rayleigh frequency range around the exact frequency value. With this procedure, the Rayleigh frequency resolution is being implicitly taken as if it were an error, or as an uncertainty estimator. However, we conducted a numerical exercise in which we fitted different sets of combination frequencies that were near the exact combination value (inside an interval of the size of the Rayleigh resolution) and we found dramatically different residuals for each of those fits, perhaps because spurious information is being introduced. Thereby, the Rayleigh resolution is not necessarily the inaccuracy associated with the determination of combination frequencies ω_k (9). The Rayleigh frequency resolution becomes a good uncertainty estimator when dealing with frequencies closer than $1/T$ to each other, but it could be exceeded when there is only one frequency component inside the Rayleigh interval.

Table 6. The 'best' parent search tree for the synthetic light-curve built from TIC 9632550 data. The first column quantifies the number of statistically significant frequencies, or children, detected with the parent frequency specified in the third column, in d^{-1} (zeros omitted for the sake of clarity). The second column is the variance after the fit of the parent and combination frequencies (in this case, only harmonics of the highest one).

No. of fitted frequencies	V value	Frequency [d^{-1}]
1	3156.591456884018044	5.0
5	948.685924387723073	5.05
14	7.165213986246192	5.055
14	7.165213986246192	5.055
14	0.804372110830800	5.05496
14	0.007417117763935	5.054964
14	0.007417117763935	5.054964
14	0.000552438323944	5.05496404
14	0.000045278362580	5.054964037
14	0.000005430569507	5.0549640372
14	0.000000546520136	5.05496403723
14	0.000000051236668	5.054964037227
14	0.000000008582531	5.0549640372273
14	**0.000000000602951**	**5.05496403722726**

It is important to note that minimizing the residuals does not guarantee that a real solution has been found. A least-squares fit, exploring all free parameters (frequencies, amplitudes and phases) without preserving the fact that the combinations are integer times the parent frequencies, can result in smaller residuals, but these cannot be explained with a closed-form formula.

5.1 Uncertainties in frequencies

The method described in this paper mainly relies on how we determine the 'best' parents. Progressively increasing the precision in frequency (when searching the minimum of the V function) involves getting closer to the floating-point number precision, which implies that numerical errors are an important source of uncertainty. Finding when these numerical effects are hampering the 'best' parents computations provides us with an estimate of the upper limit on the uncertainty of the frequencies. We find this limit by building a synthetic light-curve in this way:

$$S(t) = \sum_{k=1}^{n} A_k \cos(2\pi k\omega t + \phi_k), \quad k, n \in \mathbb{N} \tag{10}$$

where the input Fourier parameters are obtained by initially applying the method to real data, meaning that ω is the 'best' parent frequency for a mono-periodic variable up to n harmonics. Notice that there is no added noise and that the synthetic light-curve has the same number of data points as the observations. In this way, the minimum of the V function (V value) for the synthetic light-curve, theoretically expected to be zero, will reveal the error in machine calculations. The results of this test, using the components extracted from the mono-periodic δ Sct star TIC 9632550 to build the synthetic light-curve, are listed in Table 6. The 'best' parent is reached with the V value of order $\sim 6 \times 10^{-10}$. Consequently, V values smaller than this number are compromised by the numerical errors intrinsic to the machine calculations.

In addition, we divided the real light-curve of TIC 9632550 into four sections and found the 'best' parent in each of these partitions. In spite of the reduced frequency resolution, owing to the smaller time interval of the light-curve, the parent frequency found for each partition is similar, and also compatible with the O-C method up to the 4th decimal (see Table 7). This test confirms the robustness of the BPM search. In order to test if the effect of leakage had something to do with the small variation in the 4th decimal (i.e. $\sim$0.000004-s period variations), we applied the BPM to the mono-periodic light-curve with exactly an integer number of cycles and with an integer number of cycles plus half a cycle. The results of this test highlighted the influence of the number of cycles on the determination of the period. Future work could explore this issue to give a precise lower limit to the frequency uncertainty. In this regard, a conservative approach is adopted in this paper, with results expressed with the precision that the O-C method achieves.

Table 7. Results of the fundamental frequency determination by the 'best' parent search and O-C method for the four partitions of the light-curve of the mono-periodic δ Sct star TIC 9632550. Each section is $\sim$7 d long.

Section	'Best' parent [d^{-1}]	O-C frequency [d^{-1}]
S1	5.05491643	5.0548 ± 0.0001
S2	5.05490929	5.0550 ± 0.0001
S3	5.05501342	5.0549 ± 0.0002
S4	5.05501167	5.0548 ± 0.0002

As a final remark, the duration of the observation is a relevant parameter for estimating the frequency uncertainty when dealing with two close frequencies (closer than $1/T$ to each other), and so the Rayleigh frequency resolution becomes a good estimator. But, the precision can be higher than the Rayleigh frequency resolution if there is only one frequency component inside the Rayleigh interval. We just proved this for each $\sim$7-d-long section of the light-curve of the mono-periodic δ Sct star TIC 9632550. The numerical precision reached is $\pm 1 \times 10^{-8}$ and is not as if we were observing $\sim$274 000 years. The Rayleigh resolution remains the same: $\sim$1/7 d, that is, $\sim$0.14 d^{-1}.

6 CONCLUSIONS AND FUTURE WORK

Introducing spurious information to the data when fitting frequencies that do not correspond to the signal is critical for asteroseismic analyses (Balona 2014). In this work, we address this issue for the particular case in which the fitted frequencies are non-linearities. It is known that they must obey the frequency relationship that appears in equation (9). Therefore, if we know the parents, there is no need to perform a pre-whitening cascade to afterwards identify components that might (or might not) be combination frequencies (if they are near the exact value, inside a Rayleigh resolution interval) (Kurtz et al. 2015).

We have presented a method (the BPM) to compute the parent frequencies, where the optimization of the non-linear least-squares fits is done automatically and exhaustively. Regarding the numerical precision of the parents, we support a conservative approach (of the order of $\sim 10^{-5}$ d^{-1}, see Section 5.1). This is still a more realistic frequency uncertainty than the Rayleigh resolution, which, as explained above, is often implicitly used as an uncertainty to identify combination frequencies. To support the BPM, we proved that the fundamental frequency of the mono-periodic star TIC 9632550 found by the BPM is compatible with that calculated with the commonly used O-C method, known for achieving a very high precision in frequency. The extension to stars pulsating with two or more parent frequencies was also explored in this paper with positive results, in that a robust solution was found.

Moreover, this method partially overcomes the necessity to correct non-linearities in order to achieve an efficient mode identification with a linear pulsation model. Fitting combination frequencies with this method could help to identify pulsation modes by possibly revealing radial and non-radial frequency patterns, rotational splittings in the periodogram of the residuals, or just frequency and/or amplitude modulations. An example of this was shown in the results for the mono-periodic TIC 9362550, where a possible amplitude modulation was found, and in the SC observations of the HADS star KIC 5950759, where the modulating frequency ω_{m} became detectable without needing LC super-Nyquist alias analysis, as in Yang et al. (2018).

In essence we have shown that, when fitting combination frequencies of the parents yielded by the BPM, the residual light-curve is the one with the lowest contributions of these non-linearities. Unfortunately, the method does not supply a physical mechanism to explain the visibilities of the non-linearities. Results for the low-amplitude δ Sct star presented in this paper (almost no harmonics or sum combinations, but many difference combinations) provided evidence that the obtained list of statistically significant combination frequencies can be false identifications. It is true that this list might be explained by an unknown non-linear damping mechanism, by Kurtz et al.'s (2015) statement that the amplitude of children can be higher than the parents' amplitudes, by a visibility argument, or simply by coincidence in agreement with the frequency relation (9). Consequently, extra criteria for an unambiguous identification will be considered in the forthcoming Part II.

This method is shown to have a very high potential for exploring combination frequencies as the output of a non-linear system. Future research could explore the link between the theoretical foundations of this paper and the MESA (Modules for Experiments in Stellar Astrophysics) new functionality regarding non-linear radial stellar pulsations (Paxton et al. 2019), perhaps adding functionality to the data analysis pipeline of upcoming space missions (e.g. the *PLATO* mission). In the meantime, the underlying physical meaning of the generalized transfer functions Γ_j defined in equations (1) and (5) is the next step of this research. Considering orthogonal expansion in terms of a Wiener series might provide new insights into the relationships between amplitudes and phases, as first envisioned by Garrido & Rodriguez (1996). The final objective is to properly characterize the non-linear response of a pulsating star.

ACKNOWLEDGEMENTS

MLM, RGH and JPG acknowledge financial support from the State Agency for Research of the Spanish MCIU through the 'Center of Excellence Severo Ochoa' award to the Instituto de Astrofísica de Andalucía (SEV-2017-0709). The authors acknowledge funding support from Spanish public funds for research under project ESP2017-87676-C5-5-R. They thank the reviewer of this work for the advice given that helped to improve the manuscript.

DATA AVAILABILITY

The data underlying this article will be shared on reasonable request to the corresponding author.

REFERENCES

Auvergne M. et al., 2009, A&A, 506, 411
Balona L. A., 2012, MNRAS, 422, 1092
Balona L. A., 2014, MNRAS, 439, 3453
Balona L. A., 2016, MNRAS, 459, 1097
Balona L. A., Dziembowski W. A., 2011, MNRAS, 417, 591
Balona L. A. et al., 2012, MNRAS, 419, 3028
Bevington P. R., Robinson D. K., 2003, Data Reduction and Error Analysis for Physical Sciences. McGraw-Hill, New York, NY, p. 320
Bowman D. M., 2017, Amplitude Modulation of Pulsation Modes in Delta Scuti Stars. Springer International Publishing, Cham, Switzerland
Bowman D. M., Kurtz D. W., Breger M., Murphy S. J., Holdsworth D. L., 2016, MNRAS, 460, 1970
Brassard P., Fontaine G., Wesemael F., 1995, ApJS, 96, 545
Breger M., Montgomery M. H., 2014, ApJ, 783, 89
Brickhill A. J., 1992, MNRAS, 259, 519
De Franciscis S., Pascual-Granado J., Suárez J. C., García Hernández A., Garrido R., 2018, MNRAS, 481, 4637
Degroote P. et al., 2009, A&A, 506, 471
Dziembowski W. A., 1982, Acta Astron., 32, 147
Dziembowski W. A., Krolikowska M., 1985, Acta Astron., 35, 5
Dziembowski W. A., Krolikowska M., Kosovichev A. G., 1988, Acta Astron., 38, 61
Gaia Collaboration, 2018, A&A, 616, A1
García Hernández A. et al., 2013, A&A, 559, A63
Garrido R., Rodriguez E., 1996, MNRAS, 281, 696
Gillet D., Fokin A. B., 2014, A&A, 565, A73
Gilliland R. L. et al., 2010, PASP, 122, 131
Handler G. et al., 2006, MNRAS, 365, 327
Kallinger T., Reegen P., Weiss W. W., 2008, A&A, 481, 571
Kurtz D. W., Shibahashi H., Murphy S. J., Bedding T. R., Bowman D. M., 2015, MNRAS, 450, 3015
Lorimer D. R., Kramer M., 2004, Handbook of Pulsar Astronomy. Cambridge Observing Handbooks for Research Astronomers, Vol. 4. Press Syndicate of the Univ. Cambridge, Cambridge
Mantegazza L. et al., 2012, A&A, 542, A24
Montgomery M. H., 2005, ApJ, 633, 1142
Murphy S. J. et al., 2013, MNRAS, 432, 2284
Pascual-Granado J., Garrido R., Suárez J. C., 2015, A&A, 575, A78
Pascual-Granado J., Suárez J. C., Garrido R., Moya A., García Hernández A., Rodón J. R., Lares-Martiz M., 2018, A&A, 614, A40
Paxton B. et al., 2019, ApJS, 243, 10
Poretti E. et al., 2009, A&A, 506, 85
Priestley M. B., 1988, Non-linear and Non-stationary Time Series Analysis. Academic Press, London, UK
Pápics P. I., 2012, Astron. Nachrichten, 333, 1053
Reegen P., 2007, A&A, 467, 1353
Ricker G. R. et al., 2014, J. Astron. Telescopes, Instrum. Syst., 1, 014003
Saio H., Bedding T. R., Kurtz D. W., Murphy S. J., Antoci V., Shibahashi H., Li G., Takata M., 2018, MNRAS, 477, 2183
Scargle J. D., 2020, ApJ, 895, 90
Simon N. R., Lee A. S., 1981, ApJ, 248, 291
Stellingwerf R. F., 1979, ApJ, 227, 935
Sterken C., 2005, in Sterken C., ed., ASP Conf. Ser. Vol. 335, The Light-Time Effect in Astrophysics. Astron. Soc. Pac., San Francisco, p. 3
Suárez J. C., Garrido R., Pascual-Granado J., García Hernández A., de Franciscis S., Lares-Martiz M., Rodón J. R., 2020, Frontiers Astron. Space Sci., 7, 12
Van Hoolst T., 1994, A&A, 292, 471
Wiener N., 1958, Nonlinear Problems in Random Theory. MIT press, Cambridge, Massachusetts
Wu Y., 2001, MNRAS, 323, 248
Yang T. et al., 2018, ApJ, 863, 195
Zong W., Charpinet S., Fu J.-N., Vauclair G., Niu J.-S., Su J., 2018, ApJ, 853, 98
Zong W., Charpinet S., Vauclair G., Giammichele N., Grootel V. V., 2016, A&A, 585, A22

APPENDIX A: STELLAR PARAMETERS AND RELEVANT INFORMATION ON THE TIME SERIES USED

Table A1. Stellar parameters from the Gaia DR2 catalogue (Gaia Collaboration 2018) and time-series information from each space satellite. T is the length of the observation in days, and δ_t is the cadence or sampling rate in seconds. For the *TESS* and *Kepler* light-curves, we used the instrumental effects-free light-curve, resulting from the Pre-Search data Conditioning (PDC) pipeline, accessible in the Mikulski Archive for Space Telescopes (MAST: https://archive.stsci.edu/, doi:10.17909/T90K5C).

	Stellar parameters			Time series parameters		
Name	Spectral type	Magnitude m_v [mag]	Effective temp. $T_{\rm eff}$ [K]	T [d]	δ_t [s]	Obs. sequence
TIC 9632550	A8III	9.3 ± 0.1	7000^{+7200}_{-6800}	27.41	120.01	Sector 2
KIC 5950759	–	13.8 ± 0.1	7800^{+8000}_{-7600}	31.04	58.85	Quarter 4
HD 174966	A7III/IV	7.6 ± 0.1	7400^{+7600}_{-7300}	27.20	31.99	Run SRc01

APPENDIX B: COMBINATION FREQUENCIES DETECTED

Table B1. Tags of the statistically significant combination frequencies for the mono-periodic δ Sct star TIC 9632550. The frequency values can be calculated with the given parent frequencies resulting from the BPM because the fitted values are the exact combination frequency values.

Non-linearities of TIC 9362550		
2f0	7f0	12f0
3f0	8f0	13f0
4f0	9f0	14f0
5f0	10f0	
6f0	11f0	

Table B2. Tags of the statistically significant combination frequencies for the double-mode HADS star KIC 5059759. The frequency values can be calculated with the given parent frequencies resulting from the BPM because the fitted values are the exact combination frequency values.

Non-linearities of KIC 5059759					
2f0	3f0+2f1	7f0+5f1	11f0+7f1	6f0-3f1	4f1-1f0
3f0	3f0+3f1	7f0+6f1	12f0+1f1	7f0-1f1	4f1-2f0
4f0	3f0+4f1	7f0+7f1	12f0+2f1	7f0-2f1	4f1-3f0
5f0	3f0+5f1	8f0+1f1	12f0+3f1	7f0-3f1	4f1-5f0
6f0	3f0+6f1	8f0+2f1	12f0+4f1	7f0-4f1	5f1-1f0
7f0	3f0+7f1	8f0+3f1	12f0+5f1	7f0-5f1	5f1-2f0
8f0	4f0+1f1	8f0+4f1	12f0+6f1	8f0-1f1	5f1-3f0
9f0	4f0+2f1	8f0+5f1	13f0+1f1	8f0-2f1	5f1-4f0
10f0	4f0+3f1	8f0+6f1	13f0+2f1	8f0-4f1	5f1-6f0
11f0	4f0+4f1	8f0+7f1	13f0+3f1	8f0-6f1	6f1-4f0
12f0	4f0+5f1	9f0+1f1	13f0+4f1	9f0-1f1	6f1-5f0
13f0	4f0+6f1	9f0+2f1	13f0+5f1	9f0-2f1	6f1-6f0
14f0	4f0+7f1	9f0+3f1	13f0+6f1	9f0-6f1	6f1-7f0
2f1	5f0+1f1	9f0+4f1	14f0+1f1	10f0-1f1	7f1-6f0
3f1	5f0+2f1	9f0+5f1	14f0+2f1	10f0-2f1	7f1-7f0
4f1	5f0+3f1	9f0+6f1	14f0+3f1	10f0-4f1	7f1-8f0
5f1	5f0+4f1	9f0+7f1	14f0+4f1	10f0-6f1	7f1-9f0
1f0+1f1	5f0+5f1	10f0+1f1	14f0+5f1	10f0-7f1	8f1-7f0
1f0+2f1	5f0+6f1	10f0+2f1	15f0+4f1	11f0-1f1	8f1-6f0
1f0+3f1	6f0+1f1	10f0+3f1	2f0-1f1	11f0-2f1	8f1-8f0
1f0+4f1	6f0+2f1	10f0+4f1	3f0-1f1	11f0-7f1	8f1-9f0
1f0+5f1	6f0+3f1	10f0+5f1	3f0-2f1	11f0-4f1	9f1-7f0
1f0+6f1	6f0+4f1	10f0+6f1	4f0-1f1	12f0-1f1	9f1-8f0

Table B2 – *continued*

Non-linearities of KIC 5059759					
2f0+1f1	6f0+5f1	10f0+7f1	4f0-2f1	20f0-14f1	15f1-19f0
2f0+2f1	6f0+6f1	11f0+1f1	4f0-3f1	1f1-1f0	16f1-19f0
2f0+3f1	6f0+7f1	11f0+2f1	5f0-1f1	2f1-1f0	17f1-19f0
2f0+4f1	7f0+1f1	11f0+3f1	5f0-2f1	2f1-2f0	18f1-20f0
2f0+5f1	7f0+2f1	11f0+4f1	5f0-3f1	3f1-1f0	
2f0+6f1	7f0+3f1	11f0+5f1	6f0-1f1	3f1-2f0	
3f0+1f1	7f0+4f1	11f0+6f1	6f0-2f1	3f1-3f0	

Table B3. Tags of the statistically significant combination frequencies for the multi-periodic δ Sct star HD 174966. The frequency values can be calculated with the given parent frequencies resulting from the BPM because the fitted values are the exact combination frequency values.

Non-linearities of HD 174966			
2f3	6f0-5f2	9f1-9f2	8f2-7f3
1f0+1f1	7f0-6f2	1f1-1f3	9f2-6f3
1f0+1f2	8f0-6f2	3f1-2f3	9f2-7f3
1f0+1f3	9f0-6f2	3f1-5f3	1f2-1f4
1f1+1f2	9f0-7f2	4f1-3f3	3f2-1f4
1f1+1f3	9f0-8f2	6f1-4f3	4f2-2f4
1f1+2f3	2f0-1f3	7f1-6f3	4f2-3f4
1f1+1f4	3f0-2f3	9f1-8f3	4f2-4f4
2f1+1f3	5f0-2f3	3f1-3f4	5f2-4f4
2f1+1f4	5f0-4f3	4f1-2f4	6f2-3f4
1f2+1f4	5f0-5f3	4f1-4f4	6f2-4f4
1f3+1f4	7f0-4f3	5f1-4f4	7f2-4f4
1f0-1f1	7f0-5f3	6f1-5f4	7f2-6f4
2f0-1f1	8f0-5f3	7f1-6f4	8f2-6f4
3f0-1f1	8f0-6f3	8f1-6f4	8f2-8f4
3f0-3f1	2f0-2f4	8f1-7f4	8f2-9f4
5f0-4f1	2f0-3f4	8f1-8f4	9f2-7f4
6f0-3f1	3f0-1f4	1f2-1f3	9f2-8f4
6f0-5f1	4f0-3f4	2f2-1f3	1f3-1f4
7f0-6f1	4f0-4f4	3f2-2f3	1f3-2f4
8f0-5f1	5f0-2f4	4f2-3f3	2f3-1f4
8f0-8f1	7f0-4f4	5f2-2f3	2f3-3f4
9f0-7f1	8f0-6f4	5f2-3f3	3f3-1f4
9f0-8f1	1f1-1f2	5f2-4f3	4f3-4f4
1f0-2f2	1f1-2f2	5f2-5f3	5f3-4f4
1f0-3f2	3f1-3f2	6f2-4f3	5f3-5f4
4f0-3f2	5f1-6f2	6f2-5f3	6f3-5f4
5f0-3f2	6f1-7f2	7f2-6f3	6f3-6f4
5f0-4f2	7f1-7f2	7f2-7f3	
5f0-5f2	8f1-8f2	8f2-6f3	

This paper has been typeset from a TEX/LATEX file prepared by the author.